**Author for correspondence:**
Tim Connallon
e-mail: tim.connallon@monash.edu

# Local adaptation and the evolution of inversions on sex chromosomes and autosomes

Tim Connallon[1,†], Colin Olito[1,2,†], Ludovic Dutoit[3,4], Homa Papoli[3], Filip Ruzicka[5] and Lengxob Yong[6]

[1]School of Biological Sciences, and Centre for Geometric Biology, Monash University, Clayton, 3800 Victoria, Australia
[2]Department of Biology, Section for Evolutionary Ecology, Lund University, 22362 Lund, Sweden
[3]Department of Evolutionary Biology, Evolutionary Biology Centre, Uppsala University, 75236 Uppsala, Sweden
[4]Department of Zoology, University of Otago, 9054 Dunedin, New Zealand
[5]Research Department of Genetics, Evolution and Environment, University College London, London WC1E 6BT, UK
[6]Centre for Ecology and Conservation, University of Exeter, Penryn TR10 9FE, UK

TC, 0000-0002-1962-4951; CO, 0000-0001-6883-0367

Spatially varying selection with gene flow can favour the evolution of inversions that bind locally adapted alleles together, facilitate local adaptation and ultimately drive genomic divergence between species. Several studies have shown that the rates of spread and establishment of new inversions capturing locally adaptive alleles depend on a suite of evolutionary factors, including the strength of selection for local adaptation, rates of gene flow and recombination, and the deleterious mutation load carried by inversions. Because the balance of these factors is expected to differ between X (or Z) chromosomes and autosomes, opportunities for inversion evolution are likely to systematically differ between these genomic regions, though such scenarios have not been formally modelled. Here, we consider the evolutionary dynamics of X-linked and autosomal inversions in populations evolving at a balance between migration and local selection. We identify three factors that lead to asymmetric rates of X-linked and autosome inversion establishment: (1) sex-biased migration, (2) dominance of locally adapted alleles and (3) chromosome-specific deleterious mutation loads. This theory predicts an elevated rate of fixation, and depressed opportunities for polymorphism, for X-linked inversions. Our survey of data on the genomic distribution of polymorphic and fixed inversions supports both theoretical predictions.

This article is part of the theme issue 'Linking local adaptation with the evolution of sex differences'.

## 1. Introduction

Widely distributed species are often fragmented into subpopulations, each of which must cope with a unique set of abiotic stresses [1] and biotic challenges imposed by local competitor species, natural enemies, and conspecific competitors for resources and mates [2,3]. The unique conditions faced by each population generate selection for local adaptation, which favours genetic and phenotypic diversification among populations of the species, and potentially sets the stage for speciation [4–6].

Gene flow is central to the process of adaptation in fragmented populations, and has several well-known beneficial consequences: it bolsters population genetic diversity, alleviates harmful effects of genetic drift and inbreeding depression, and increases the evolutionary capacity of populations within the species' range [7–9]. On the other hand, gene flow also inhibits genetic divergence between populations, and thereby constrains their potential to locally adapt. The establishment and maintenance of local adaptations depends on the balance between gene flow and local selection [4,10]. Even under the best circumstances, sustained migration results in perpetual maladaptation in populations receiving

†Denotes equal contributions.

**THE ROYAL SOCIETY** PUBLISHING

**Box 1.** Processes of inversion evolution.

Comparative genomic studies show that closely related species exhibit extensive differences in gene order, and these differences arise through the spread of inversions (e.g. [26,27]). Although the specific processes accounting for inversion fixation are not well known, four general processes potentially contribute. These include: (1) genetic drift; (2) positive selection on beneficial inversions; (3) linked positive selection on inversions that carry beneficial genetic variation; and (4) segregation distortion in favour of inversions over wild-type chromosomes. We provide a brief overview of these scenarios below. Readers seeking a broader review of theory and empirical examples should consult the references [23,28,29].

*Genetic drift of (nearly) neutral and under-dominant inversions.* Neutral and slightly deleterious inversions may fix solely by genetic drift [29]. Under-dominant inversions—in which inversion heterozygotes have reduced fitness relative to homozygotes of inversion and wild-type chromosomes—become fixed by a combination of genetic drift and positive selection; drift can allow an initially rare inversion to reach a high enough frequency in the population for positive selection to subsequently drive it to fixation [30,31].

*Positive selection of beneficial inversions.* An inversion may directly improve fitness of its carriers by favourably altering the expression of genes within the inversion, or of genes that flank inversion break points [23,29]. Standard evolutionary models for adaptive substitution can be applied in such cases, including evolutionary models contrasting X-linked and autosome divergence [22,30].

*Indirect positive selection due to linkage.* Selection can favour inversions that become associated with beneficial genetic variation, though the inversion is not beneficial *per se*. Inversions may spread within the population if they carry alleles within them that are individually beneficial [23], or epistatically beneficial in combination [32]. Inversions may also spread when they are free of deleterious alleles that are maintained within the population by recurrent mutation [33], or by maladaptive gene flow from other regions of the species' range [23]. Our models focus on the latter two scenarios, which are illustrated in figure 1.

*Meiotic drive.* Inversions can spread within the population if they become associated with meiotic drive, i.e. in heterozygotes for inversion and wild-type chromosomes, the preferential meiotic segregation of inversions into gametes. Whether a driving inversion eventually becomes fixed will also depend on whether it is saddled with deleterious fitness consequences in individuals homozygous for the inversion (as in the Segregation Distorter or SD system in *Drosophila* [34]), or the inversion causes sex-ratio distortion [35]. In both cases, selection against the inversion will intensify as it increases in frequency in the population, limiting its likelihood of fixation.

migrants [11,12]. In the worst-case scenario, populations can collapse as a consequence of the 'swamping' of local adaptation by strong gene flow [13,14].

The extent to which gene flow constrains adaptation varies across the genome. Loci differ in their phenotypic effects on traits targeted by local selection, leading to heterogeneity among genes in their contributions to population differentiation [15,16]. Moreover, some regions of the genome are inherently less susceptible than others to the swamping effects of gene flow, which may lead to predictable genomic architectures of local adaptation [17]. The genetic basis of local adaptation and species divergence may involve 'islands' of genetic differentiation within a genomic sea of undifferentiated loci [18], and unequal contributions of different chromosome types to genetic divergence [19–22].

Local selection also favours the evolution of genome structural changes that bind locally beneficial alleles together and eliminate recombination between them [15,17,19]. For example, inversions that capture sets of locally adaptive alleles can spread within a population because they reduce recombination with 'migrant' chromosomes that harbour locally maladaptive alleles [23–25]. In an influential theoretical study, Kirkpatrick & Barton [23] showed that inversions spread under a wide range of contexts of local selection with gene flow. Moreover, a single population genetic parameter—the migration rate—defines a population's potential for inversion evolution during local adaptation; provided the loci captured by an inversion were not tightly linked to begin with (see [24,25]), the establishment probability of an inversion is proportional to the migration rate of locally maladapted individuals into the population [23].

A range of evolutionary scenarios can potentially trigger the evolutionary spread and fixation of new inversions (box 1). Most models—including current theories of inversion evolution during local adaptation—focus on autosomal inheritance, where the dynamics of inversions and of local adaptation depend on the average intensity of selection and migration in females and males of the species. By contrast, the evolutionary dynamics of sex chromosomes are heavily influenced by sex differences in selection, mutation, migration, recombination and demography, which collectively lead to fundamentally different patterns of evolution at autosomal and X-linked genes [36,37]. These sex differences are widespread [38] and can lead to different contributions of the X and autosomes to: (i) genetic admixture and population differentiation [20,39,40], (ii) molecular population genetic diversity and divergence between species [22,41], and (iii) genetic variation for fitness [42–44]. Although previous models have considered the spread of X-linked inversions with under-dominant fitness effects (see [30]) and inversions promoting divergence between sex chromosomes (between the X and Y, or the Z and W; see [45–47]), current theory has so far ignored the role of sex linkage in the evolution of locally adapted inversions. This is somewhat surprising given the extensive development of theory on the individual roles of inversions and X-linked inheritance in adaptation and speciation [22,48–50], as well as the wealth of inversion data that is currently available for species with sex chromosomes [26,28,30,51,52].

Here, we extend Kirkpatrick & Barton's [23] model for the evolution of locally adapted inversions, and characterize the relative rates of establishment of inversions on the X and autosomes. We focus on the impacts of sexual dimorphism in
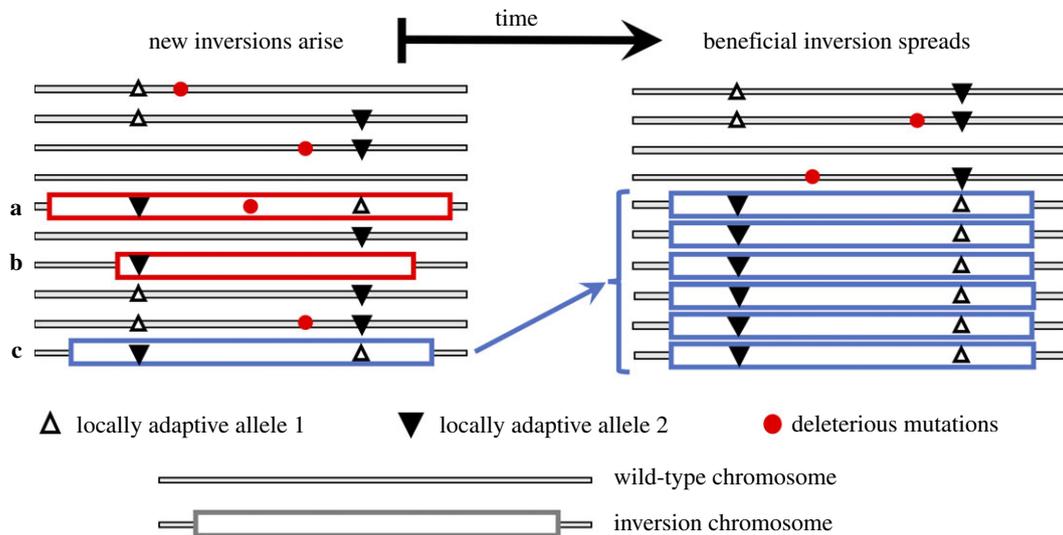
**Figure 1.** The spread of an inversion that captures a high-fitness genetic background. The cartoon illustrates the consequences of two forms of genetic variation on the evolution of inversions. The left and right panels each represent a sample of chromosomes from a population at two different points in time. Two loci (locus 1 and locus 2) segregate for locally adaptive alleles (marked as triangles) evolving at migration – selection balance. The remaining sites within the region segregate for deleterious alleles evolving at mutation – selection balance (red circles). The left-hand panel represents a population primarily comprising wild-type chromosomes, with rare inversions that each capture a random set of locally adaptive and/or deleterious alleles. Inversions marked in red are eventually purged from the population because they capture a deleterious mutation (the inversion labelled 'a'), or fail to capture both locally adaptive alleles (the inversion labelled 'b'). Such inversions suppress recombination with wild-type chromosomes and are, therefore, forever burdened by the suboptimal genotypes that they initially capture. The blue inversion (labelled 'c') is favoured by natural selection because it is mutation-free and it binds together the locally adaptive alleles by suppressing recombination between them. In the right-hand panel, the beneficial inversion has spread, while the deleterious inversions have been removed from the population.

mutation, selection and migration on the evolutionary dynamics of inversions, as well as the consequences of local adaptation for the evolution of structural changes in different regions of the genome (figure 1). Our aim is to identify drivers of inversion evolution on the X and autosomes, and conditions leading to different rates of inversion accumulation on each chromosome type. Finally, we evaluate predictions of our models by reviewing current empirical data on polymorphic and fixed inversions on sex chromosomes and autosomes.

## 2. Material and methods

Our analytical framework follows that of Kirkpatrick & Barton [23], who characterized the evolutionary dynamics of rare inversions in a focal population receiving a steady flow of migrants from a much larger external population. Following their model, we assume that loci responding to local selection have independent effects on fitness (i.e. there is no epistasis between loci). Generations are non-overlapping and migration and selection parameters are small (see below for details). Prior to the origin of inversions, recombination between loci is high relative to the strength of selection per locus. We refer readers to Charlesworth & Barton [25] for a rigorous analysis of inversion dynamics under arbitrary linkage. Our simulations relax many of our analytical assumptions and allow us to explore effects of tight linkage on inversion dynamics.

We present models focusing on contrasts between X-linked and autosomal inversions, though our results also apply to species with Z-linked inheritance, in which females represent the heterogametic sex (the equivalent to males in species with X chromosomes). All of our models focus on species with heteromorphic sex chromosomes, where X-linked and Z-linked genes are haploid in the heterogametic sex. Although we do not consider the evolution of locally adapted inversions in species with undifferentiated (homomorphic) sex chromosomes (see

[53]), we note that the dynamics of such inversions should be similar to those of autosomal inversions, with the added consequence that X-linked and Z-linked inversions that span the sex-determination region would suppress recombination on Y and W chromosomes, and thereby promote differentiation and degeneration between homomorphic X and Y, or Z and W, chromosome pairs.

## (a) Migration – selection balance prior to the origin of inversions

In each generation, a fixed proportion of females and males are migrants: $m_f$ and $m_m$, respectively. Accounting for the relative contributions of maternal and paternal genetic transmission to the inheritance of autosomal and X-linked genes, the *effective* migration rates for autosomes and the X, respectively, are $m_A = \frac{1}{2}(m_f + m_m)$ and $m_X = \frac{1}{3}(2m_f + m_m)$ [20,38].

Each locus (arbitrarily labelled locus $i$) has two alleles: an $A_i$ allele which is fixed in the external population, and $a_i$ which is favoured in the focal population. Locally adapted alleles increase fitness by $s_{if}$ and $s_{im}$ in female and male homozygotes, and $s_{if}h_i$ and $s_{im}h_i$ in heterozygotes, where $h_i$ is the dominance coefficient for the $i$th locus ($0 < h_i < 1$, with $h_i < \frac{1}{2}$ corresponding to partial recessivity of the locally adaptive allele, $h_i > \frac{1}{2}$ to partial dominance and $h_i = \frac{1}{2}$ to additivity; we assume there are no sex differences in dominance); see table 1 for a complete list of model notation used throughout the paper.

Following Charlesworth & Charlesworth ([54] ch. 4), when migration and selection parameters are small (e.g. $1 \gg s_{if}, s_{im}$; $1 \gg m_A, m_X$), the equilibrium frequency of a maladaptive allele at an autosomal locus can be approximated as

$$\hat{q}_i = \frac{(1-h_i)}{2(1-2h_i)}\left(1 - \sqrt{1 - \frac{8(1-2h_i)m_A}{(1-h_i)^2(s_{if}+s_{im})}}\right)$$

$$\approx \frac{2m_A}{(1-h_i)(s_{if}+s_{im})} \tag{2.1a}$$

**Table 1.** Summary of notation.

| | |
|---|---|
| f, m | sex: f = female; m = male |
| $L, l$ | sets of loci evolved at migration–selection balance |
| $m_f, m_m$ | sex-specific migration rates |
| $m_A, m_X$ | effective migration rate per autosome ($m_A$) and X-linked locus ($m_X$) |
| $s_{if}, s_{im}$ | sex-specific selection coefficient in favour of the $i$th locally adaptive allele |
| $h_i$ | dominance coefficient of the $i$th locally adaptive allele |
| $n$ | the number of loci evolved at migration–selection balance within an inversion |
| $\bar{t}_A, \bar{t}_X$ | average effective strength of selection against locally maladaptive alleles on the autosomes ($\bar{t}_A$) and X chromosome ($\bar{t}_X$) |
| $\lambda_A, \lambda_X$ | invasion fitness of rare autosomal ($\lambda_A$) and X-linked ($\lambda_X$) inversions |
| $s_I$ | selection on a rare inversion |
| $u_{if}, u_{im}$ | sex-specific mutation rates at the $i$th locus at mutation–selection balance |
| $s_{d,if}, s_{d,im}$ | sex-specific selection coefficients of the deleterious mutation at the $i$th locus at mutation–selection balance |
| $h_{d,i}$ | dominance coefficient of the deleterious mutation at the $i$th locus at mutation–selection balance |
| $\alpha$ | ratio of male and female mutation rates ($u_{im}/u_{if}$) |
| $\beta$ | ratio of male and female selection coefficients of deleterious mutations ($s_{d,im}/s_{d,if}$) |
| $U_f$ | female total deleterious mutation rate per inversion |
| $u_i$ | effective mutation rate for the $i$th locus at mutation–selection balance: $u_i = (u_{if} + u_{im})/2$ for an autosomal locus; $u_i = (2u_{if} + u_{im})/3$ for an X-linked locus |
| $d_i$ | effective strength of selection at the $i$th locus at mutation–selection balance: $d_i = h_{d,i}(s_{d,if} + s_{d,if})/2$ for an autosomal locus; $d_i = (2h_{d,i} s_{d,if} + s_{d,im})/3$ for an X-linked locus |

and the equilibrium for an X-linked locus is

$$\hat{q}_i = \frac{(2s_{if}(1 - h_i) + s_{im})}{4s_{if}(1 - 2h_i)}\left(1 - \sqrt{1 - \frac{8s_{if}(1 - 2h_i)3m_X}{(2s_{if}(1 - h_i) + s_{im})^2}}\right)$$
$$\approx \frac{3m_X}{2s_{if}(1 - h_i) + s_{im}} \tag{2.1b}$$

(see the electronic supplementary material, Appendix I). The final approximations, which we use extensively in the analytical results, imply that locally maladaptive alleles are rare within the focal population. These approximations are valid when selection against locally maladaptive alleles in heterozygotes is strong relative to the migration rate ($s_{ij}(1 - h_i) \gg m_A, m_X$); the more exact results apply for arbitrary migration relative to selection.

## (b) Selection on rare inversions

The expected rate of increase of a rare inversion depends on the marginal fitness associated with the inversion compared to the mean fitness of all genotypes in the population. Kirkpatrick & Barton [23] modelled inversion dynamics within a focal population that experiences one-way migration from a source population in which the alleles that are locally maladaptive for the focal population are fixed. Here, the invasion fitness of a rare inversion within the focal population is

$$\lambda = (1 + s_I) = (1 - m)\frac{W_I}{\bar{W}}, \tag{2.2}$$

where $s_I$ is the rate of frequency change for a rare inversion in a deterministically evolving population (essentially, the selection coefficient for a rare inversion; see [25]), $m$ is the rate of migration, $W_I$ is the marginal fitness of the inversion and $\bar{W}$ is the mean fitness of the population. Selection favours the inversion's spread within the population when $\lambda > 1$ ($s_I > 0$); selection acts against the inversion when $\lambda < 1$ ($s_I < 0$).

To account for sex-linked inheritance and sex differences in selection and migration, we modify equation (2.2) as

follows (see the electronic supplementary material, Appendix II). Invasion fitness of a rare autosomal inversion becomes

$$\lambda_A \approx (1 - m_A)\left(\frac{W_{If}}{2\bar{W}_f} + \frac{W_{Im}}{2\bar{W}_m}\right), \tag{2.2a}$$

where the f and m subscripts distinguish the marginal and mean fitnesses of each sex. Invasion fitness of an X-linked inversion becomes

$$\lambda_X \approx (1 - m_X)\left(\frac{2}{3}\frac{W_{If}}{\bar{W}_f} + \frac{1}{3}\frac{W_{Im}}{\bar{W}_m}\right). \tag{2.2b}$$

These expressions take into account the fractions of autosomal and X-linked genes that are maternally and paternally inherited, and follow standard population genetics theory for autosomal and X-linked evolutionary dynamics under weak selection [36,55] (see the electronic supplementary material, Appendix II).

Kirkpatrick & Barton [23] further developed approximations for $W_I$ and $\bar{W}$ in equation (2.2), which apply when the ancestral rate of recombination between loci is high relative to the strength of selection for local adaptation at individual loci (see [25]). We extend their approach to incorporate effects of sex-specific selection and X-linked inheritance. Consider a new inversion that captures locally adaptive alleles at a set of $L$ loci within the larger set of $I$ total loci that span the inversion. Under the stated assumptions (weak selection and migration; loose linkage between loci in the ancestral population; no epistasis), female selection on an autosomal or X-linked inversion is given by

$$\frac{W_{If}}{\bar{W}_f} = \frac{\prod_{i\in L}[1 + s_{if}(1 - \hat{q}_i(1 - h_i))]\prod_{i\in(I-L)}[1 + s_{if}h_i(1 - \hat{q}_i)]}{\prod_{i\in I}[1 + s_{if}(1 - \hat{q}_i)(1 - \hat{q}_i(1 - 2h_i))]}. \tag{2.3a}$$

The above equation also applies for male selection on an autosomal inversion (i.e. $W_{Im}/\bar{W}$, with m subscripts replacing f

subscripts in equation (2.3a)). Male selection under X-linked inheritance is

$$\frac{W_{Im}}{\bar{W}_m} = \frac{\prod_{i \in L}(1 + s_{im})}{\prod_{i \in I}(1 + s_{im}(1 - \hat{q}_i))}.$$  (2.3b)

Approximations of equations (2.3a) and (2.3b), used in the main analytical results below, are provided in the electronic supplementary material, Appendix III.

## (c) The distribution of fitness effects and establishment probability of new inversions

When many loci segregate independently at migration–selection balance, and each has a small effect on fitness, we can approximate the distribution of fitness effects and establishment probabilities of new X-linked or autosomal inversions that span a given set of loci at migration–selection balance, and that capture a random sample of locally adaptive and maladaptive alleles within the set of loci (see the electronic supplementary material, Appendix III).

With many independent loci, each having a small fitness effect, the distribution of fitness effects of random inversions (the distribution of $s_I$) will be approximately normal with mean and variance of $\bar{s}_I$ and $\sigma^2$, respectively (see the electronic supplementary material, Appendix III). Assuming that the population size is large and selection coefficients are small ($1 \gg |s_I| \gg 1/N$, where $N$ is the population size), inversion establishment probabilities are approximately $2s_I$ when $s_I > 0$ and zero otherwise (e.g. [56]). The probability of inversion establishment is

$$\left.\begin{array}{l} \Pi = \int_0^\infty 2s_I f(s_I)ds_I = \bar{s}_I\left[1 - \mathrm{erf}\left(-\frac{\bar{s}_I}{\sqrt{2\sigma^2}}\right)\right] + \sqrt{\frac{2\sigma^2}{\pi}}\exp\left(-\frac{\bar{s}_I^2}{2\sigma^2}\right) \\[4mm] = \bar{s}_I + \sqrt{\frac{2\sigma^2}{\pi}} + O(\bar{s}_I^2), \end{array}\right\}$$  (2.4)

where $f(s_I)$ is the probability density function for inversion selection coefficients (see the electronic supplementary material, Appendix III).

## (d) Simulations

To complement our analytical results, we carried out stochastic simulations to rigorously explore the behaviour of a two-locus version of the model, with arbitrary ancestral linkage between them. Exact recursions follow the life cycle: (1) birth, (2) selection, (3) migration, (4) recombination and random mating of adults and (5) death. The recombination rate between loci was $r_f$ and $r_m$ for females and males, respectively, with no X-linked recombination in males.

For each simulation run, we iterated deterministic recursions to convergence to the exact migration–selection equilibrium for the two-locus system with the inversion absent from the population. We then introduced a single copy of an inversion that captured locally adaptive alleles at both loci, and carried out Wright-Fisher forward simulations using the deterministic recursions and multinomial sampling of genotype frequencies for each sex among a pool of $N$ breeding adults, per generation. For simplicity, we assume a constant number of adults in each generation with an equal sex ratio (i.e. selection is 'soft' in that the size of the focal population is independent of its genetic composition). Each simulation run lasted until the inversion was lost from the population or crossed a threshold frequency ($p = p^*$) that corresponds to an establishment probability of $\approx 0.9997$, where $p^* = 2/(Nm_A)$ for the autosome model and $p^* = 8/(3Nm_X)$ for the X. To confirm that successfully established inversions eventually increase towards fixation, we carried out additional simulations for $4N$ generations, allowing sufficient time for inversions to approach fixation. Complete simulation code can be found at https://github.com/colin-olito/XvAutosomeInversions.

# 3. Results and discussion

Our results and discussion are divided into four major sections. First, we provide a full characterization of the simplest version of our model: the evolution of an inversion that spans two loci and captures the locally adaptive alleles at both. We explore how dominance and partial linkage between loci affect the establishment of X-linked and autosomal inversions. Second, we explore the dynamics of rare inversions spanning many loci, where each locus has a small effect on local adaptation. Here, establishment probabilities of new inversions take into account the different proportions of locally adaptive and maladaptive alleles that are captured by X-linked versus autosomal inversions. Third, we consider how X/autosome differences in the standing load of deleterious mutations affect the establishment of inversions on each chromosome type. Finally, we review data on X-linked and autosomal inversions, and discuss the relation between empirical patterns and predictions of our models.

## (a) Two-locus evolutionary dynamics

Previous theory has shown that when selection is strong relative to migration and locally adaptive loci are loosely linked in the ancestral population, the rate of spread of a rare inversion that captures the locally adaptive alleles is proportional to the migration rate [23–25]. In the electronic supplementary material, Appendix III, we show that these conclusions apply under both autosomal and X-linked inheritance. With two loci at migration–selection balance, selection coefficients for rare inversions that capture locally adapted alleles at both loci ($s_I$) are

$$s_{I,A} = \lambda_A - 1 \approx m_A + O(m_A^2)$$  (3.1a)

and

$$s_{I,X} = \lambda_X - 1 \approx m_X + O(m_X^2),$$  (3.1b)

for autosomal and X-linked inversions, respectively. With weak migration (i.e. ignoring higher-order terms of $m_X$ and $m_A$), the establishment probabilities of autosomal and X-linked inversions will be $\Pi_A \approx 2s_{I,A} \approx 2m_A$ and $\Pi_X \approx 2s_{I,X} \approx 2m_X$, respectively, and sex-specific migration patterns determine the *relative* establishment probabilities of inversions. With no sexual dimorphism in migration, establishment probabilities will be equal between the X and autosomes ($m_A = m_X$). Male-biased migration leads to a higher establishment probability on autosomes, and female-biased migration causes a higher probability on the X. In the extremes—with sex-limited migration—autosomal establishment probabilities are 50% higher when males are the migrating sex ($\Pi_A/\Pi_X \approx 3/2$); X-linked probabilities are approximately 33% higher when females are the migrating sex ($\Pi_A/\Pi_X \approx 3/4$).

The approximations in equations (3.1a) and (3.1b) compare well with more exact numerical results using equations (2.1) and (2.2), and evaluated across the full range of dominance for locally adaptive alleles (figure 2a). Equations (3.1a) and (3.1b) also perform well against stochastic simulations of inversion establishment, as long as selection for local adaptation is weak relative to the ancestral recombination rate between loci (i.e. $r \gg s$, as predicted by previous theory [25]; figure 2b; electronic supplementary material, figure S1). The simulations confirm that $2m_A$ and $2m_X$ provide useful approximations for inversion establishment probabilities under loose linkage in the ancestral population (as predicted in [23,25]). In addition,
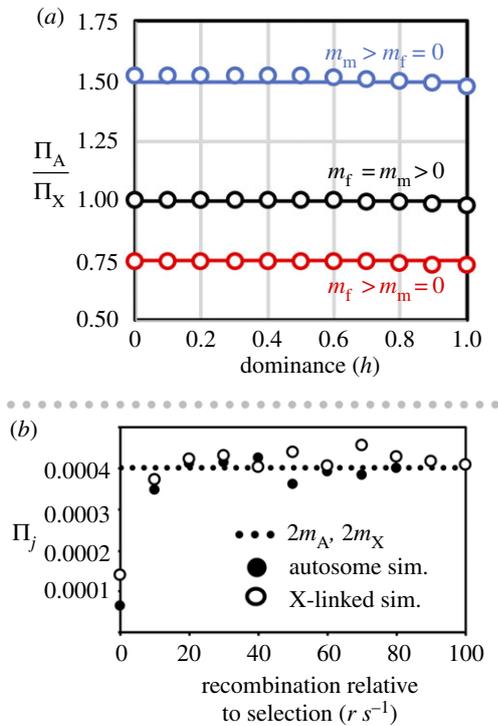
5

6

rstb.royalsocietypublishing.org    Phil. Trans. R. Soc. B 373: 20170423



**Figure 2.** Effects of dominance and recombination on the establishment of inversions that capture two locally adapted alleles. (*a*) Effects of dominance on selection for rare inversions. Solid lines show the ratio of X and autosome approximations, based on equations (3.1*a*) and (3.1*b*), for three idealized scenarios of sex-specific migration: male-limited migration (blue), equal migration (black) and female-limited migration (red); open circles show numerical evaluation of exact equations (2.1) and (2.2), with $(s_f + s_m)/2 = 0.1$, and $(m_f + m_m)/2 = 0.01$, and a dominance coefficient of $h = h_i$ at both loci. (*b*) A representative comparison between analytical approximations for X and autosome establishment probabilities (broken line, based on equations (3.1*a*) and (3.1*b*), with $m_f = m_m$) and stochastic simulations of inversion establishment in a Wright-Fisher population of size $N = 500\,000$, with $s = s_f = s_m = 0.005$, $m_f = m_m = 0.0002$, and sex-specific recombination rates of $r = r_f = r_m$ with no X-linked recombination in males; $j$ refers to the mode of inheritance ($j = \{A, X\}$). Each circle shows the fraction of $10^6$ single-copy inversions that eventually become established in the population. Analytical, numerical and simulation results are based on the two-locus model of local adaptation in which inversions capture locally adaptive alleles at both loci. For additional simulation results, see electronic supplementary material, figures S1 and S2.

inversions that successfully invade the population will ultimately approach fixation (electronic supplementary material, figure S2).

## (b) Inversions spanning many loci with small fitness effects

The above results are conditioned on X-linked and autosomal inversions capturing equal numbers of locally adaptive alleles. In reality, new inversions are expected to capture a random set of alleles at the loci that they span, and some may be locally maladaptive. To consider effects of random allele sampling on inversion establishment, we consider newly arising inversions that capture an arbitrary set of locally adaptive alleles at the loci that the inversion spans. Each inversion spans a specific set of $I$ loci (either on the X or on an autosome), and each locus within the set $I$ segregates

at migration–selection balance equilibrium. $L$ represents the set of loci in an inversion ($L$ is a subset of $I$) that carry the locally adaptive allele.

With many segregating loci, each with small fitness effects and loose ancestral linkage between them, the distribution of fitness effects of new autosomal inversions is approximately normal with mean and variance of $\bar{s}_I \approx -m_A$ and $\sigma^2 \approx n m_A \bar{t}_A$, where $n$ is the number of loci within the inversion and $\bar{t}_A$ is the average heterozygous fitness cost of a maladaptive allele (the average value of $\frac{1}{2}(s_{if} + s_{im})(1 - h_i)$ for the set of loci in the inversion; see the electronic supplementary material, Appendix III). Under X-linked inheritance, the mean and variance of new inversion fitness effects will be $\bar{s}_I \approx -m_X$ and $\sigma^2 \approx n m_X \bar{t}_X$, where $\bar{t}_X$ is the average value of $\frac{1}{3}[2s_{if}(1 - h_i) + s_{im}]$ (see the electronic supplementary material, Appendix III). By incorporating these expressions into equation (2.4), we obtain the ratio of establishment probabilities for new autosomal versus new X-linked inversions:

$$\frac{\Pi_A}{\Pi_X} \approx \frac{m_A\left(\sqrt{2n\bar{t}_A/\pi m_A} - 1\right)}{m_X\left(\sqrt{2n\bar{t}_X/\pi m_X} - 1\right)} \approx \sqrt{\frac{m_A\bar{t}_A}{m_X\bar{t}_X}}, \quad (3.2)$$

with the last approximation applicable when $\bar{t}_A$, $\bar{t}_X \gg m_A$, $m_X$ (as we assume throughout). Equation (3.2) reveals that the establishment probabilities depend on an interaction between dominance, sex-biased migration and sex-specific selection. Each factor influences the pre-inversion equilibrium frequencies of locally adaptive alleles, and thereby mediates the distributions of adaptive and maladaptive alleles captured by random inversions.

To evaluate the effects of dominance and sex-specific selection and migration on $\Pi_A/\Pi_X$, we suppose that dominance is constant among loci ($h = h_i$), and the distribution of selection coefficients ($s_{if}$ and $s_{im}$) is equal between chromosomes. With selection equal between the sexes, equation (3.2) simplifies to $\Pi_A/\Pi_X \approx \sqrt{3m_A(1 - h)}/\sqrt{m_X(3 - 2h)}$. Under male-limited selection, we get $\Pi_A/\Pi_X \approx \sqrt{3m_A(1 - h)}/\sqrt{2m_X}$; and with female-limited selection, we get $\Pi_A/\Pi_X \approx \sqrt{3m_A}/\sqrt{4m_X}$. These results are plotted in figure 3, which shows that $\Pi_A/\Pi_X$ declines with the dominance of locally adaptive alleles, provided there is some selection through males ($\Pi_A/\Pi_X$ is unaffected by dominance when selection is limited to females). This makes intuitive sense: with increased masking of migrant alleles, maladaptive alleles reach higher equilibrium frequencies on autosomes, and X-linked inversions capture larger proportions of locally adaptive alleles and become established more readily than autosomal inversions.

## (c) Deleterious mutations and inversion dynamics

New inversions can vary in the proportions of locally adaptive alleles that they capture, as well as their loads of deleterious mutations. Deleterious mutations can hinder the spread of inversions by dampening or overwhelming positive selection arising in the context of local adaptation. As deleterious alleles typically reach different equilibrium frequencies on the X and autosomes, they may disproportionately affect inversion dynamics on the two chromosome types. As the bulk of deleterious mutations are expressed in heterozygotes [57,58], we first consider the effects of incompletely recessive mutations on the establishment probabilities of X-linked and autosomal inversions. We later consider how completely recessive mutations potentially impact the dynamics of autosomal inversions.
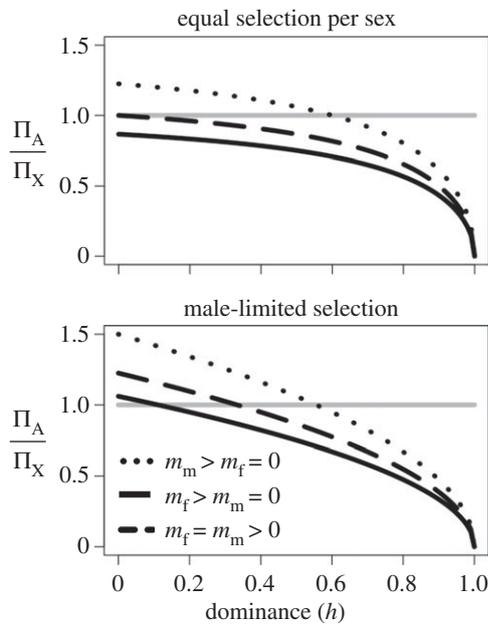
**Figure 3.** Establishment probabilities of autosomal and X-linked inversions that span many loci with small effects on local adaptation. Curves show the special cases of equation (3.2) (see text following equation (3.2)), which assume that dominance of locally adaptive alleles is constant across the set of loci captured by the inversion ($h = h_i$), and distributions of selection coefficients among loci are the same for the X and autosomes ($\bar{t}_X = \bar{t}_A$). Values greater than one correspond to higher establishment probabilities for autosomal inversions; values less than one correspond to greater X-linked establishment probabilities.

### (i) Incompletely recessive deleterious mutations

To characterize the effects of deleterious mutations on establishment of X-linked and autosomal inversions, we focus on the simplest case where each inversion captures only locally adaptive alleles at a set of $n$ loci that were loosely linked prior to the origin of the inversion (as before, selection and migration are assumed to be weak). We suppose that the inversion also spans a set of loci at mutation–selection balance equilibrium; there is no epistasis or linkage disequilibrium between the deleterious mutations. Nei et al. [33] previously considered the evolution of inversions that are favoured because they carry fewer mutations than most other haplotypes in the population. Following their model, we assume that inversions cannot invade the population unless they are free of deleterious mutations; this assumption is reasonable as long as the benefit of the inversion for local adaptation and the cumulative mutation rate across loci are both modest (i.e. less than $s_d h_d$, the heterozygous fitness cost of a deleterious mutation; see [33]). Following standard theory, mutation–selection equilibrium at a locus $i$ is $q_i^* \sim u_i/d_i$, where $u_i$ is the mutation rate and $d_i$ is the effective strength of purifying selection against deleterious alleles at the locus ($d_i \gg u_i$). Chromosome-specific definitions for $u_i$ and $d_i$ are provided in table 1.

In the electronic supplementary material, Appendix IV, we derive selection coefficients for a rare inversion that is free of deleterious mutations and that captures only the locally adaptive alleles at all $n$ loci at migration–selection balance. After also taking into account the probability that random inversions carry no deleterious mutations, we obtain a general expression for the relative probability of establishment for autosomal
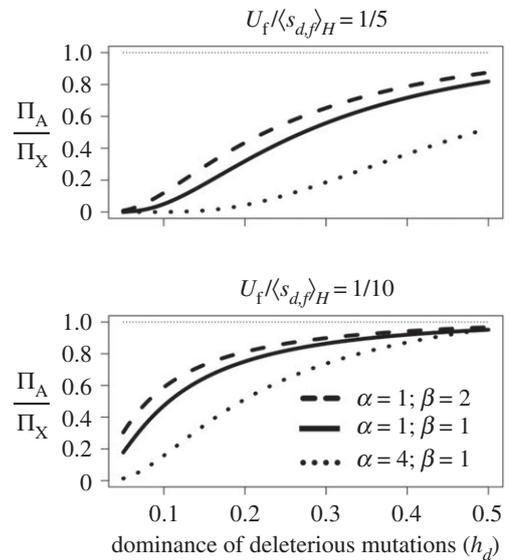


**Figure 4.** Deleterious mutations dampen establishment probabilities of autosomal inversions. The y-axis shows how deleterious mutations reduce the establishment probability of autosomal inversions relative to those on the X. Results are based on equation (3.3), with $\alpha = u_{im}/u_{if}$, $\beta = s_{d,im}/s_{d,if}$, $U_f = 0.01$, $m_A(n-1) = m_X(n-1) = 0.01$.

versus X-linked inversions:

$$\frac{\Pi_A}{\Pi_X} \approx \exp\left(\frac{U_f}{\langle s_{d,f}\rangle_H}\left[\frac{2+\alpha}{2h_d+\beta}-\frac{1+\alpha}{h_d(1+\beta)}\right]\right)\frac{U_f\frac{1}{2}(1+\alpha)+m_A(n-1)}{U_f\frac{1}{3}(2+\alpha)+m_X(n-1)},$$
(3.3)

where $\langle s_{d,f}\rangle_H$ is the harmonic mean deleterious selection coefficient in females, $U_f$ is the total rate of mutation in females (i.e. across the set of mutation–selection balance loci within an inversion). For simplicity, equation (3.3) assumes that dominance coefficients and ratios of sex-specific mutation and selection parameters are constant across loci ($h_{d,i} = h_d$; $\alpha = u_{im}/u_{if}$, $\beta = s_{d,im}/s_{d,it}$).

Evaluation of equation (3.3) shows that deleterious mutations within inversions can severely dampen the probability of inversion establishment, with deleterious mutations having a greater impact on autosomal than X-linked inversions (figure 4). The greater impact of deleterious mutations on autosomal inversions reflects the higher load of deleterious mutations carried by autosomes compared to the X, and consequently, the lower probability that a given autosomal inversion will be mutation-free. In the simplest case, where mutation, selection and migration parameters are equal between the sexes, $\Pi_A/\Pi_X$ is always less than one—and establishment probabilities are greater on the X—across the entire plausible range of dominance ($0 < h_d < 1$; see the electronic supplementary material, Appendix IV). The quantitative discrepancy between inversions on the X and autosomes can be substantial: $\Pi_A/\Pi_X$ is likely to be small when mutation rates are male-biased ($\alpha > 1$) and deleterious mutations are partially recessive ($h_d < 0.5$, as shown in figure 4). Modest sex differences in the fitness effects of deleterious mutations (see [59,60]) have a comparatively small impact on the results.

### (ii) Recessive deleterious mutations

Although the vast majority of mutations are partially expressed in heterozygotes (with $h_d \sim 1/4$, on average; see [57,58]), a small subset of deleterious alleles is completely recessive.

Because recessive mutations are completely masked in hetero-zygotes, they will not hinder the initial spread of autosomal inversions, which may ultimately become established even when they carry one or more strongly deleterious recessive alleles. Such inversions will not fix because their spread is eventually counteracted by selection against low-fitness homo-zygotes of the inversion, which express the full fitness cost of deleterious mutations [23]. This mechanism for inversion poly-morphism is unfeasible for X-linked inversions because X-linked recessives are fully expressed in males.

Assuming that completely recessive mutations have no impact on the establishment of autosomal inversions, the fraction of autosomal inversions that carry one or more recessive deleterious alleles may be approximated as

$$G \approx 1 - \exp\left(-\frac{\sqrt{U_0}}{\langle\sqrt{s_d}\rangle_H}\right), \qquad (3.4)$$

(electronic supplementary material, Appendix IV), where $U_0$ is the total mutation rate to recessive deleterious alleles within the region that the inversion spans and $\langle\sqrt{s_d}\rangle_H$ is the harmonic mean of the square root of selection coefficients for recessive mutations. To get a sense of how large $G$ is likely to be, we con-sider the extreme case of recessive lethal mutations ($s_d = 1$), where estimates from *Drosophila* suggest a lethal mutation rate of $U_0 = 0.006$ per chromosome per generation [61]. Equation (3.4) provides an upper limit for this case: approximately 8% of large (chromosome-spanning) autosomal inversions capture recessive lethals; this proportion should decrease for smaller inversions. However, if we take into account non-lethal reces-sives—those causing sterility, or having milder fitness effects—then the 8% benchmark could underestimate the true fraction of autosomal inversions that carry one or more deleterious reces-sive alleles. Such inversions may invade the population when rare, and persist as polymorphisms maintained by associative overdominance (see [23]).

## (d) Comparison between theoretical predictions and inversion data

Our models predict that three factors should influence the evolutionary accumulation of inversions on sex chromosomes relative to autosomes. Compared to autosomes, the higher efficacy of selection at X- and Z-linked genes is expected to increase the frequencies of locally adapted alleles and decrease the load of deleterious mutations. As a result, sex-linked inversions tend to 'capture' higher-fitness genotypes, and experience higher establishment probabilities. Sex-biased migration can modify these predictions somewhat, with higher migration in the homogametic sex (e.g. females in XX/XY species) increasing inversion biases towards the sex chromosomes; higher migration in the heterogametic sex should decrease the bias. Finally, because recessive deleterious alleles are more likely to generate associative overdominance on autosomes, we predict a higher proportion of polymorphic inversions on the autosomes compared to the X or Z.

We conducted a review of the chromosomal locations of inversions by searching the literature for evidence of poly-morphic and fixed inversions. Much of the data were obtained from reviews of cytological data [30,52] and taxon-specific comparative genomics datasets [27,51]. We expanded the data collection beyond these studies by searching Google Scholar and Pubmed for relevant search terms (inver-sion, rearrangement, polymorphism, fixed, polytene, local
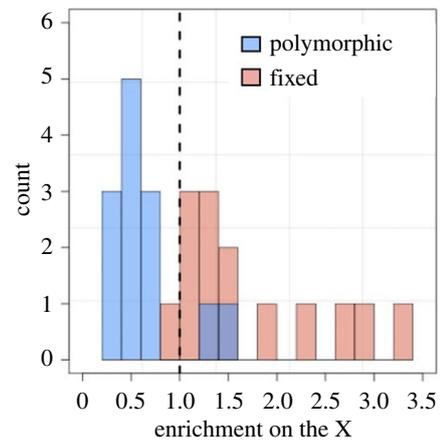


**Figure 5.** The X chromosome contains more inversions than expected relative to its size when considering fixed between-species differences. However, it contains fewer within-species polymorphic inversions. Each bar represents the ratio of the proportion of X-linked inversions to the proportion of auto-somal inversions (i.e. fold enrichment on the X), scaled by the corresponding chromosome size for each species, or species pair (for polymorphic and fixed inversions, respectively). Data can be found in electronic supplementary material, tables S1 and S2. We have excluded species where fewer than 10 inversions are known.

adaptation, sex chromosomes, autosomes) in conjunction with clade names where known genomic or cytological studies have been conducted. As sex chromosomes and autosomes make up different proportions of the genome, and these pro-portions vary among species, we focused on the numbers of polymorphic and fixed inversions on each chromosome type, relative to their proportional contributions to the genome. All data refer to paracentric inversions unless otherwise stated.

Two clear patterns emerged from the inversion data. First, fixed inversions show consistent enrichment on X and Z chromosomes relative to their sizes (electronic supplementary material, table S1; figure 5), which is consistent with our theor-etical predictions. Analysis of 12 *Drosophila* genomes suggests an approximately 1.2-fold enrichment of fixed inversions on the X [27,62], which corroborates previous observations of X-linked enrichment for fixed inversions in *Drosophila* and other insects [30]. Likewise, across 16 species of *Anopheles* mosquitoes, rearrangement rates are approximately 2.7 times higher on the X relative to autosomes [51]. The X also shows an excess of fixed inversions between humans and chimpan-zees compared to similarly sized autosomes [63]. Finally, across 81 clades of passerine birds, Hooper and Price [52] report that pericentric inversions fix at a rate approximately 1.4 times higher on the Z chromosome relative to autosomes.

Second, although data on inversion polymorphisms are less readily available than those on fixed inversions, species from which data are sufficient to contrast the X and auto-somes suggest that polymorphic inversions are typically more common on autosomes (electronic supplementary material, table S2; figure 5). This pattern could reflect our pre-diction that segregating autosomal inversions can harbour recessive deleterious mutations that generate balancing selec-tion via associative overdominance. A recent high-resolution genomic analysis of *Drosophila melanogaster* shows no bias between the X and autosomes, relative to their proportions of the genome [26]; of 27 inversions detected, 22% are X-linked, corresponding to the approximately 18% of the genome that is X-linked. However, extensive cytological

data from the *Drosophila* and *Anopheles* clades show a clear excess of polymorphic inversions on autosomes.

## 5. Conclusion

We have shown that the evolutionary fates of inversions differ when they arise on sex chromosomes versus autosomes. In our model, inversions are favoured because they facilitate local adaptation, and inversion establishment probabilities are typically higher on the X (or Z) than on autosomes. This sex chromosome bias is strongest when migration is higher in the homogametic sex, locally adapted alleles are strongly expressed in heterozygotes, and inversions are large enough to span many loci evolving at migration–selection and mutation–selection balance (as is widely observed in classical cytology data, e.g. [30,52]). Deleterious mutations appear to have the strongest impact on the dynamics of X-linked and autosomal inversions; the higher burden of deleterious mutations on autosomes can impose a strong constraint to the invasion and fixation of autosomal inversions. These predictions are consistent with empirical patterns of fixed and polymorphic inversions (figure 5).

The observed excess of fixed inversions on X and Z chromosomes most probably reflects the greater efficiency of purifying selection on X and Z chromosomes (i.e. against locally maladaptive or unconditionally harmful alleles). Several lines of empirical evidence, spanning genomics to quantitative genetics data, suggest that sex linkage facilitates the removal of deleterious genetic variation (e.g. [37,59,64]). The possible role of sex-biased migration in inversion evolution is less clear. Data on sex-specific migration in arthropods are sparse, though mark–recapture studies in *Drosophila* suggest that sex-specific migration may range from female-biased to male-biased in the genus [65–69]. It has long been recognized that migration rates are typically higher for the heterogametic sex in birds and mammals (i.e. females and males, respectively [70]), which should, if anything, dampen the preferential accumulation of inversions on Z and X chromosomes. A fine-scaled phylogenetic comparative analysis of correlations between the degree of sex-biased migration and the magnitude of inversion bias towards the X or Z would help clarify the impact of migration on genomic patterns of inversion accumulation.

While our models provide a compelling explanation for empirical patterns of fixed and polymorphic inversions on sex chromosomes and autosomes, they do not preclude the role of other factors in driving non-random genomic patterns of inversion evolution. Several other mechanisms, including positive selection on inversions, meiotic drive and fixation of under-dominant inversions by genetic drift, may also contribute to inversion evolution (see box 1), and each mechanism may play out differently on the X and autosomes. Direct, positive selection on inversions (e.g. due to position effects of genes) could lead to a faster-X pattern if inversions are intrinsically beneficial and partially recessive [22,30,71]. Under-dominant inversions are more likely to fix on the X than the autosomes, because directional selection in males on X-linked inversions can overwhelm any under-dominant fitness costs to heterozygous females [22]. Finally, idiosyncratic features of sex chromosome composition, including repeat abundance, may lead to mutational biases in the formation of new inversions [62,72]. High-resolution data on polymorphic and fixed inversions, along with tests of neutrality for inversion polymorphisms [73] may help shed further light on these possibilities.

## References

1. Siepielski AM et al. 2017 Precipitation drives global variation in natural selection. *Science* **355**, 959–962. (doi:10.1126/science.aag2773)

2. Schluter D. 2000 *The ecology of adaptive radiation*. Oxford, UK: Oxford University Press.

3. Kawecki TJ, Ebert D. 2004 Conceptual issues in local adaptation. *Ecol. Lett.* **7**, 1225–1241. (doi:10.1111/j.1461-0248.2004.00684.x)

4. Endler JA. 1977 *Geographic variation, speciation, and clines*. Princeton, NJ: Princeton University Press.

5. Coyne JA, Orr HA. 2004 *Speciation*. Sunderland, MA: Sinauer Associates.

6. Nosil P. 2012. *Ecological speciation*. Oxford, UK: Oxford University Press.

7. Alleaume-Benharira M, Pen IR, Ronce O. 2006 Geographical patterns of adaptation within a species' range: interactions between drift and gene flow. *J. Evol. Biol.* **19**, 203–215. (doi:10.1111/j.1420-9101.2005.00976.x)

8. Whiteley AR, Fitzpatrick SW, Funk WC, Tallmon DA. 2015 Genetic rescue to the rescue. *Trends Ecol. Evol.* **30**, 421–449. (doi:10.1016/j.tree.2014.10.009)

9. Frankham R. 2015 Genetic rescue of small inbred populations; meta-analysis reveals large and consistent benefits of gene flow. *Mol. Ecol.* **24**, 2610–2618. (doi:10.1111/mec.13139)

10. Yeaman S, Otto SP. 2011 Establishment and maintenance of adaptive genetic divergence under migration, selection, and drift. *Evolution* **65**, 2123–2129. (doi:10.1111/j.1558-5646.2011.01277.x)

11. Moran PAP. 1962 *The statistical process of evolutionary theory*. Oxford, UK: Oxford University Press.

12. García-Ramos G, Kirkpatrick M. 1997 Genetic models of adaptation and gene flow in peripheral populations. *Evolution* **51**, 21–28. (doi:10.1111/j.1558-5646.1997.tb02384.x)

13. Kirkpatrick M, Barton NH. 1997 Evolution of a species' range. *Am. Nat.* **150**, 1–23. (doi:10.1086/286054)

14. Polechová J, Barton NH. 2015 Limits to adaptation along environmental gradients. *Proc. Natl Acad. Sci. USA* **112**, 6401–6406. (doi:10.1073/pnas.1421515112)

15. Yeaman S. 2013 Genomic rearrangements and the evolution of clusters of locally adaptive loci. *Proc. Natl Acad. Sci. USA* **11**, E1743–E1751. (doi:10.1073/pnas.1219381110)

16. Yeaman S. 2015 Local adaptation by alleles of small effect. *Am. Nat.* **186**, S74–S89. (doi:10.1086/682405)

17. Yeaman S, Whitlock MC. 2011 The genetic architecture of adaptation under migration-selection

balance. *Evolution* **65**, 1897–1911. (doi:10.1111/j.1558-5646.2011.01269.x)

18. Wolf JBW, Ellegren H. 2017 Making senese of genomic islands of differentiation in light of speciation. *Nat. Rev. Genet.* **18**, 87–100. (doi:10.1038/nrg.2016.133)

19. Kirkpatrick M. 2010 How and why chromosome inversions evolve. *PLoS Biol.* **8**, e1000501. (doi:10.1371/journal.pbio.1000501)

20. Lasne C, Sgrò CM, Connallon T. 2017 The relative contributions of the X chromosome and autosomes to local adaptation. *Genetics* **205**, 1285–1304. (doi:10.1534/genetics.116.194670)

21. Camus MF, Wolff JN, Sgrò CM, Dowling DK. 2017 Experimental support that natural selection has shaped the latitudinal distribution of mitochondrial haplotypes in Australian *Drosophila melanogaster*. *Mol. Biol. Evol.* **34**, 2600–2612. (doi:10.1093/molbev/msx184)

22. Charlesworth B, Campos JL, Jackson BC. In press. Faster-X evolution: theory and evidence from *Drosophila*. *Mol. Ecol.*

23. Kirkpatrick M, Barton N. 2006 Chromosome inversions, local adaptation and speciation. *Genetics* **173**, 419–434. (doi:10.1534/genetics.105.047985)

24. Bürger R, Akerman A. 2011 The effects of linkage and gene flow on local adaptation in a continent-island model. *Theor. Pop. Biol.* **80**, 272–288. (doi:10.1016/j.tpb.2011.07.002)

25. Charlesworth B, Barton NH. 2018 The spread of an inversion with migration and selection. *Genetics* **208**, 377–382. (doi:10.1534/genetics.117.300426)

26. Chakraborty M, VanKuren NW, Zhao R, Zhang X, Kalsow S, Emerson JJ. 2018 Hidden genetic variation shapes the structure of functional elements in *Drosophila*. *Nat. Genet.* **50**, 20–25. (doi:10.1038/s41588-017-0010-y)

27. Bhutkar A, Schaeffer SW, Russo SM, Xu M, Smith TF, Gelbart WM. 2008 Chromosomal rearrangement inferred from the comparisons of 12 *Drosophila* genomes. *Genetics* **179**, 1657–1680. (doi:10.1534/genetics.107.086108)

28. Wellenreuther M, Bernatchez L. 2018 Eco-evolutionary genomics of chromosomal inversions. *Trends Ecol. Evol.* **33**, 427–440.

29. Hoffmann AA, Reiseberg LH. 2008 Revisiting the impact of inversions in evolution: from population genetic markers to drivers of adaptive shifts and speciation? *Annu. Rev. Ecol. Evol. Syst.* **39**, 21–42. (doi:10.1146/annurev.ecolsys.39.110707.173532)

30. Charlesworth B, Coyne JA, Barton NH. 1987 The relative rates of sex chromosomes and autosomes. *Am. Nat.* **130**, 113–145. (doi:10.1086/284701)

31. Lande R. 1979 Effective deme sizes during long-term evolution estimated from rates of chromosomal rearrangements. *Evolution* **33**, 234–251. (doi:10.1111/j.1558-5646.1979.tb04678.x)

32. Feldman MW, Otto SP, Christiansen FB. 1997 Population genetic perspectives on the evolution of recombination. *Annu. Rev. Genet.* **30**, 261–295. (doi:10.1146/annurev.genet.30.1.261)

33. Nei M, Kojima K, Schaffer HE. 1967 Frequency changes of new inversions in population

under mutation-selection balance. *Genetics* **57**, 741–750.

34. Larracuente AM, Presgraves DC. 2012 The selfish *Segregation Distorter* gene complex of *Drosophila melanogaster*. *Genetics* **192**, 33–53. (doi:10.1534/genetics.112.141390)

35. Jaenike J. 2001 Sex chromosome meiotic drive. *Annu. Rev. Ecol. Syst.* **32**, 25–49. (doi:10.1146/annurev.ecolsys.32.081501.113958)

36. Avery PJ. 1984 The population genetics of haplo-diploids and X-linked genes. *Genet. Res. Camb.* **44**, 321–341. (doi:10.1017/S0016672300026550)

37. Vicoso B, Charlesworth B. 2006 Evolution of the X chromosome: unusual patterns and processes. *Nat. Rev. Genet.* **7**, 645–653. (doi:10.1038/nrg1914)

38. Hedrick PW. 2007 Sex: differences in mutation, recombination, selection, gene flow, and genetic drift. *Evolution* **61**, 2750–2771. (doi:10.1111/j.1558-5646.2007.00250.x)

39. Goldberg A, Rosenberg NA. 2015 Beyond 2/3 and 1/3: the complex signatures of sex-biased admixture on the X chromosome. *Genetics* **201**, 263–279. (doi:10.1534/genetics.115.178509)

40. Webster TH, Wilson Sayres MA. 2016 Genomic signatures of sex-biased demography: progress and prospects. *Curr. Opin. Genet. Dev.* **41**, 62–71. (doi:10.1016/j.gde.2016.08.002)

41. Charlesworth B. 2009 Fundamental concepts in genetics: effective population size and patterns of molecular evolution. *Nat. Rev. Genet.* **10**, 195–205. (doi:10.1038/nrg2526)

42. Pamilo P. 1979 Genic variation at sex-linked loci: quantification of regular selection models. *Hereditas* **91**, 129–133. (doi:10.1111/j.1601-5223.1979.tb01652.x)

43. Patten MM, Haig D. 2009 Maintenance or loss of genetic variation under sexual and parental antagonism at a sex-linked locus. *Evolution* **63**, 2888–2895. (doi:10.1111/j.1558-5646.2009.00764.x)

44. Connallon T. 2010 Genic capture, sex linkage, and the heritability of fitness. *Am. Nat.* **175**, 564–576. (doi:10.1086/651590)

45. Lenormand T. 2003 The evolution of sex dimorphism in recombination. *Genetics* **163**, 811–822.

46. Otto SP. 2014 Selective maintenance of recombination between the sex chromosomes. *J. Evol. Biol.* **27**, 1431–1442. (doi:10.1111/jeb.12324)

47. Blackmon H, Brandvain Y. 2017 Long-term fragility of Y chromosomes is dominanted by short-term resolution of sexual antagonism. *Genetics* **207**, 1621–1629. (doi:10.1534/genetics.117.300382)

48. Presgraves DC. 2008 Sex chromosomes and speciation in *Drosophila*. *Trends Genet.* **24**, 336–343. (doi:10.1016/j.tig.2008.04.007)

49. Meisel RP, Connallon T. 2013 The faster-X effect: integrating theory and data. *Trends Genet.* **29**, 537–544. (doi:10.1016/j.tig.2013.05.009)

50. Muirhead CA, Presgraves DC. 2016 Hybrid incompatibilities, local adaptation, and the genomic distribution of natural introgression between

species. *Am. Nat.* **187**, 249–261. (doi:10.1086/684583)

51. Neafsey DE et al. 2015 Highly evolvable malaria vectors: the genomes of 16 *Anopheles* mosquitoes. *Science* **347**, 1258522. (doi:10.1126/science.1258522)

52. Hooper DM, Price TD. 2017 Chromosomal inversion differences correlate with range overlap in passerine birds. *Nat. Ecol. Evol.* **1**, 1526–1534. (doi:10.1038/s41559-017-0284-6)

53. Bachtrog D et al. 2014 Sex determination: why so many ways of doing it? *PLoS Biol.* **12**, e1001899. (doi:10.1371/journal.pbio.1001899)

54. Charlesworth B, Charlesworth D. 2010 *Elements of evolutionary genetics*. Greenwood Village, CO: Roberts and Company.

55. Nagylaki T. 1979 Selection in dioecious populations. *Ann. Human Genet.* **43**, 143–150. (doi:10.1111/j.1469-1809.1979.tb02007.x)

56. Haldane JBS. 1927 A mathematical theory of natural and artificial selection. Part V. Selection and mutation. *Proc. Camb. Phil. Soc.* **23**, 838–844. (doi:10.1017/S0305004100015644)

57. Manna F, Martin G, Lenormand T. 2011 Fitness landscapes: an alternative theory for the dominance of mutation. *Genetics* **189**, 923–937. (doi:10.1534/genetics.111.132944)

58. Charlesworth B. 2015 Causes of natural variation in fitness: evidence from studies of *Drosophila* populations. *Proc. Natl Acad. Sci. USA* **112**, 1662–1669. (doi:10.1073/pnas.1423275112)

59. Mallet MA, Bouchard JM, Kimber CM, Chippindale AK. 2011 Experimental mutation-accumulation on the X chromosome of *Drosophila melanogaster* reveals stronger selection on males than females. *BMC Evol. Biol.* **11**, 156. (doi:10.1186/1471-2148-11-156)

60. Sharp NP, Agrawal AF. 2013 Male-biased fitness effects of spontaneous mutations in *Drosophila melanogaster*. *Evolution* **67**, 1189–1195. (doi:10.1111/j.1558-5646.2012.01834.x)

61. Halligan DL, Keightley PD. 2009 Spontaneous mutation accumulation studies in evolutionary genetics. *Annu. Rev. Ecol. Evol. Syst.* **40**, 151–172. (doi:10.1146/annurev.ecolsys.39.110707.173437)

62. von Grotthuss M, Ashburner M, Ranz JM. 2010 Fragile regions and not functional constraints predominate in shaping gene organization in the genus *Drosophila*. *Genome Res.* **20**, 1084–1096. (doi:10.1101/gr.103713.109)

63. Feuk L, MacDonald JR, Tang T, Carson AR, Li M, Rao G, Khaja R, Scherer SW. 2005 Discovery of human inversion polymorphisms by comparative analysis of human chimpanzee DNA sequence assemblies. *PLoS Genet.* **1**, e56. (doi:10.1371/journal.pgen.0010056)

64. Eanes WF, Hey J, Houle D. 1985 Homozygous and hemizygous viability variation on the X chromosome of *Drosophila melanogaster*. *Genetics* **111**, 831–844.

65. McKenzie JA. 1974 The distribution of vineyard populations of *D. melanogaster* and *D. simulans* during vintage and non-vintage periods. *Oecologia* **15**, 1–16. (doi:10.1007/BF00345225)

66. Powell JR, Dobzhansky T, Hook JE, Wistrand H. 1976 Genetics of natural populations. XLIII. Further studies on rates of dispersal of *D. pseudoobscura* and its relatives. *Genetics* **82**, 495–506.

67. Begon M. 1976 Dispersal density and microdistribution in *Drosophila subobscura*. *J. Anim. Ecol.* **45**, 441–456. (doi:10.2307/3884)

68. Fontedevilla A, Carson H. 1978 Spatial distribution and dispersal in a population of *Drosophila*. *Am. Nat.* **112**, 365–394. (doi:10.1086/283279)

69. Markow TA, Castrezana S. 2000 Dispersal in cactophilic *Drosophila*. *Oikos* **89**, 378–386. (doi:10.1034/j.1600-0706.2000.890219.x)

70. Trochet A, Courtois EA, Stevens VM, Baguette M, Chaine A, Schmeller DS, Clobert J. 2016 Evolution of sex-biased dispersal. *Q. Rev. Biol.* **91**, 297–320. (doi:10.1086/688097)

71. Connallon T, Singh ND, Clark AG. 2012 Impact of genetic architecture on the relative rates of X versus autosomal adaptive substitution.

*Mol. Biol. Evol.* **29**, 1933–1942. (doi:10.1093/molbev/mss057)

72. Hooper DM, Price TD. 2015 Rates of karyotypic evolution in Estrildid finches differ between island and continental clades. *Evolution* **69**, 890–903. (doi:10.1111/evo.12633)

73. Corbett-Detig RB, Hartl DL. 2012 Population genomics of inversion polymorphism in *Drosophila melanogaster*. *PLoS Genet.* **8**, e1003056. (doi:10.1371/journal.pgen.1003056)

11

rstb.royalsocietypublishing.org    *Phil. Trans. R. Soc. B* **373**: 20170423